LAWRENCE
LIVERMORE
NATIONAL
LABORATORY

LLNL-PROC-656400

Binder Mixing and Concentration Variation in TATB Polymer-Bound Explosives

T. M. Willey, L. Lauderbach, G. Overturf

July 2, 2014

International Detonation Symposium
San Francisco, CA, United States
July 14, 2014 through July 18, 2014

Disclaimer

Binder Mixing and Concentration Variation in TATB Polymer-Bound Explosives

Trevor M. Willey, Lisa Lauderbach, Franco Gagliardi, and George Overturf

Lawrence Livermore National Laboratory, Livermore, CA 94550

A survey of various lots of TATB (1,3,5-tri-amino-2,4,6- tri-nitrobenzene) mixed with 5-7.5% Kel-F 800 binder reveals a lot-dependent variation in how homogenously the binder mixes with the explosive in pressed materials. Monochromatic x-ray microtomography quantitatively reveals the microstructure and volume constituent concentrations and thus the extent of binder/TATB mixing variation. The technique, outlined here, is particularly applicable to explosive-binder mixtures where the explosive and binder possess dramatically different attenuation coefficients, for example, when the binder contains higher atomic weight elements (e.g. Cl) or is of a dramatically different density.

Introduction

TATB (1, 3, 5 - tri-amino- 2, 4, 6 - tri-nitrobenzene) is a highly insensitive energetic material often mixed with polymer binders[1] to improve mechanical properties and enable pressing to high density. Two common formulations, LX-17 and PBX-9502, use Kel-F 800 (poly chlorotrifluoroethylene-co-vinylidene fluoride) as a binder with nominal concentrations of 7.5% and 5%, respectively. Samples investigated with tomography were previously observed to have a variation in binder concentration of about 1.5% on mm length scales[2, 3] with binder-rich regions surrounding binder poor regions. The so-called prill structure is consistent with the formulation of these explosives where mm-sized spheres, or prills, form during the mixing of binder and explosive prior to pressing.

This observation motivates several questions: What is the cause of this variation? Does it result purely from the formulation step? How does the production lot of TATB or Kel-F 800 contribute to the degree of heterogeneity? Can homogeneous LX-17 and/or PBX-9502 be reliably synthesized? And ultimately, what are the possible impacts of heterogeneity, if any, on mechanical and detonation properties? These questions, beyond the scope of this paper, cannot be addressed or answered without first understanding the degree of microstructural variation.

The goals of this paper are thus to quantitatively characterize TATB / Kel-F 800 homogeneity in high explosives, and to demonstrate the utility of synchrotron-based computed tomography to quantitatively determine composition of 3D volumes in explosive-binder mixtures. To this end, synchrotron-based tomography was performed on over 50 samples of LX-17 and PBX-9502 with different lots, pressings, and ages represented – a starting point towards answering the above questions. The data, which is directly importable and/or comparable to modeling, could also give insight into how explosive/binder heterogeneity affects mechanical and/or detonation properties.

Methods

Synchrotron-based x-ray computed microtomography enables quantitative determination of constituent volume fractions, voxel by voxel, in three-dimensional volumes of explosive-binder mixtures like LX-17 and PBX-9502. Using monochromatic incident x-rays, the well-defined, well-known, and energy dependent attenuation coefficients μ[4] can be directly compared to resultant measured μ from reconstructed slices. As an example, at 20 keV, TATB and Kel-F 800 have attenuation coefficients of 1.1 and 4.1 cm^{-1} respectively; at 30 keV, these are 0.5 and 1.4 cm^{-1}. In the simple case of a mixture of two materials (e.g. TATB and Kel-F 800) these differences and nonlinearity in μ as a function of energy enable volume fraction determination through the linear relationships $V_{TATB} \cdot \mu_{TATB} + V_{KelF} \cdot \mu_{KelF} = \mu_{measured}$ at two energies, and $V_{TATB} + V_{KelF} + V_{void} = 1$. This can be extended to N materials (including void), requiring N-1 acquisitions, each at a unique energy. At length scales presented, void volume generally is less than a few percent and varies little with a slight increase with decreasing binder concentration [2, 3]. The voxel size used is larger than the expected TATB crystallite sizes and thus each voxel should represent a macroscopic volume, i.e. each voxel volume should encompass a number of TATB crystallites with associated binder and void, whereas at much smaller length scales, one might expect a voxel of one material only. The Kel-F 800 (and thus TATB) concentration can also be estimated from a single energy acquisition by assuming a void distribution as a function of μ.

Based on several multi-energy acquisitions that show void volume tracks mildly with TATB volume concentration (and inversely with Kel-F 800 concentration) coupled with the small change in void volume (~0.1% over twice the fwhm of the distribution in voxel linear attenuation coefficients) we chose a distribution of void matching this criteria. Over the vast majority of voxels, this is essentially a linear relationship. Also, at the extremes one would expect void distribution in the extreme case to approach 100% as μ approaches zero, and void volume to approach 0% at large μ. A rotated hyperbola fits these criteria and was used for the single energy approximation.

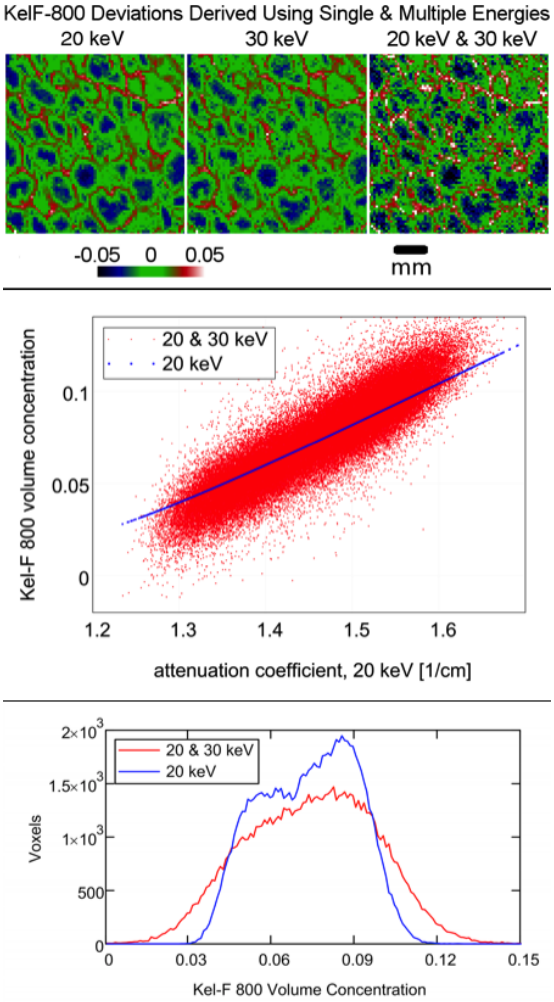

Figure 1: Comparison between derivation of Kel-F 800 concentration deviation from nominal from single acquisitions (20 keV & 30 keV) vs. dual energy with no assumption on void distribution. Top panes present slices, mid-pane Kel-F 800 concentration vs. 20 keV attenuation coefficient, and histograms from the single-energy 20 keV acquisition vs. the dual energy method.

The differences between single and dual energy scans are presented in Fig. 1. The upper right and upper middle panes present slices at 71.2

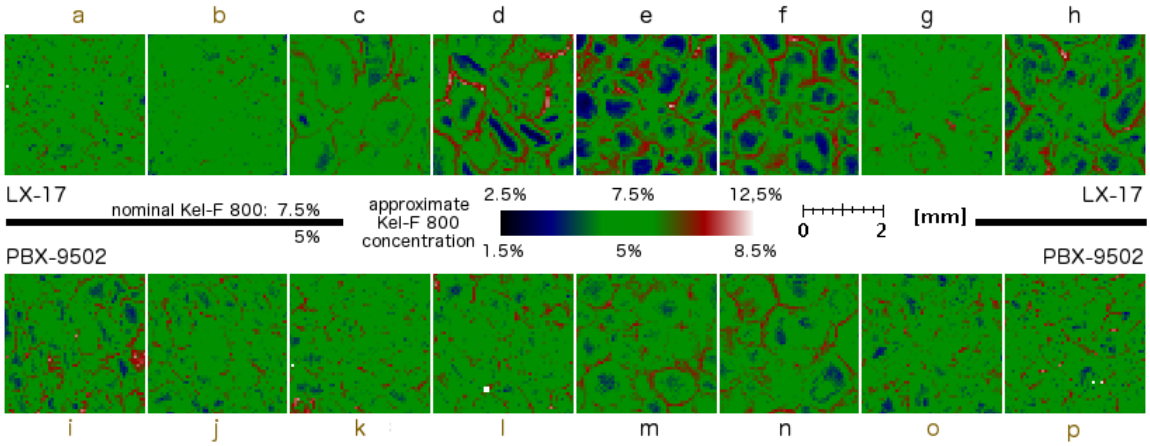

Figure 2: Slices depicting deviation from nominal Kel-F 800 concentration derived from x-ray computed tomography. Different batches (lots) of LX-17 are presented on the top row, and of PBX-9502 on the bottom row.

micron resolution, of the deviation from the nominal Kel-F 800 concentration (~7.5% by weight) using the single-energy approach at 20 keV and 30 keV, respectively. The upper right pane presents this deviation in Kel-F 800 concentration derived from both the 20 and 30 keV acquisitions using the linear relationships presented above and not assuming a void distribution. The multi-energy slice clearly possesses the lowest signal to noise of the series, followed by the 30 keV scan. The lower signal to noise of the 30 keV scan is expected due to the high, and non-optimal, > 50% transmission at this energy. Errors from both the 20keV and 30 keV scans contribute to the multi-energy slice; the middle and lower panes estimate this error. The middle pane presents the Kel-F concentrations, for each of the ~10^5 voxels in this particular volume, plotted vs. its attenuation coefficient at 20 keV. The blue points lie on a single curve as expected, while the concentrations for the multi-energy are distributed red points. Plotting the distribution of the difference between the multi- and 20 keV concentration leads to a Gaussian distribution with fwhm of 0.9%. Conversely, a similar calculation with the 30 keV data vs. the 20 keV data gives a Gaussian with fwhm of 0.4%, a measure of error between these two, as the single-energy scans would be expected to give nearly identical results. Although the multi-energy data is more accurate, this is eclipsed by its lack of precision (minimally 0.4%) at these length scales and acquisition parameters. Perhaps the most interesting trend arises from simply the visual inspection of the data. The blue 20 keV computed slope underestimates the approximate slope of the red multi-energy data, and thus indicates the single-energy approximation, if anything, slightly underestimates the degree of inhomogeneity. The bottom pane plots the histogram of Kel-F 800 volume concentration for the 20 keV single energy, and multi-energy data. Both show a double peak structure reminiscent of early CT work on LX-17 distinguishing a binder-rich prill boundary region and a binder-poor prill interior. The multi-energy peaks are somewhat broader than the single; at least 0.4% is random errors as described above. The similar shape and broadness indicates that the single-energy method is a reasonable approximation to obtain Kel-F 800 concentrations in these explosives.

Results

Figure 2 presents slices of the approximate Kel-F 800 concentration from within the interior of LX-17 and PBX-9502 samples of

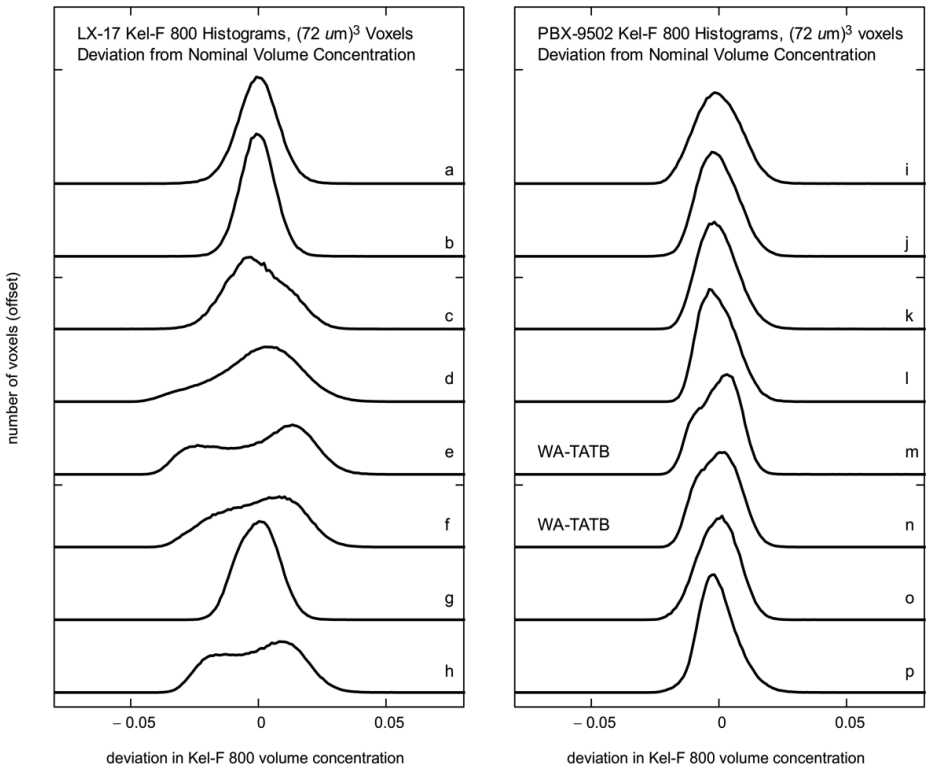

Figure 3: Histograms of the deviation in Kel-F 800 concentration from nominal.

different manufacturing lots, labeled a through p. The variation in Kel-F 800 concentration is only dependent upon lot: Several samples from within single batches possess similar binder inhomogeneity irrespective of conditioning (i.e. temperature cycling[5], age, or mechanical creep). LX-17 lots a and b are most homogeneous, c and g are moderately homogeneous, and d, e, f, and h are heterogeneous. PBX-9502 lots are moderately homogeneous, with lots m and n being most heterogeneous. Having established the heterogeneity is purely lot-dependent, the most apparent predictor of inhomogeneity to date is whether dry-aminated, or wet-aminated TATB was used in the formulation. Brown letters in Fig. 2 (e.g. LX-17 lots a and b) indicate formulations using dry-aminated TATB, while black (e.g. PBX-9502 lots m and n) are made with wet-aminated TATB. The dry-aminated lots lead to slices that are qualitatively more homogeneous than wet-aminated from inspection of the slices in Fig.1. Conversely, lots made with wet-aminated TATB have prill boundaries; this observation is supported by the histogram data of Fig. 3. Wet aminated TATB leads to broader, asymmetric, and often bimodal histograms. No wet-aminated histograms are as narrow as dry-aminated for LX-17, and the wet-aminated histograms of lots m and n are the only peaks exhibiting bimodal structure in the PBX-9502.

Although the use of wet- vs. dry-aminated TATB is the most apparent factor influencing degree of inhomogeneity, the TATB type is not the only parameter, and may even be coincidental with other process changes. The variation observed within the lots formulated with wet-aminated TATB indicates other factors affect the binder/TATB mixing. The microstructure varies from grossly heterogeneous in e to relatively homogeneous in g. The histogram from g, however, is still broader than the LX-17 formed with dry aminated TATB.

These data will also be interesting starting points to compare mechanical and detonation

properties to binder/explosive mixing. For example, studies now comparing binder homogeneity to mechanical strength, or TATB concentration to localized detonation properties are now possible. The three-dimensional data can also be used as direct input to modeling.

Summary and Conclusions

Quantitative three-dimensional compositional volumes can be obtained via monochromatic x-ray computed tomography. Generally, N multiple acquisitions at different energies can discriminate the volume concentration of N well-known constituents. In the case presented here, the constituents of TATB, Kel-F 800 binder (and void) are discriminated. For voids that here encompass a small portion of the volume and have a somewhat known distribution, a reasonable approximation is to assume a void volume distribution as a function of attenuation coefficient, and then use a single acquisition to determine TATB and Kel-F 800 volume concentration.

These CT datasets for LX-17 and PBX-9502 are crucial starting point as empirical experimental input to high fidelity computational models, and in understanding how microstructure affects subtle detonation and mechanical property differences in TATB-based explosives.

Acknowledgements

The authors thank D. Parkinson, ALS, LBNL, for assistance during tomography experiments. Lawrence Livermore National Laboratory is operated by Lawrence Livermore National Security, LLC, for the U.S. Department of Energy, National Nuclear Security Administration under Contract DE-AC52-07NA27344. The Advanced Light Source is supported by the Director, Office of Science, Office of Basic Energy Sciences, of the U.S. Department of Energy under Contract No. DE-AC02-05CH11231. LLNL-PROC-656400.

References

1. Willey, T.M., D.M. Hoffman, T. van Buuren, L. Lauderbach, J. Ilavsky, R.H. Gee, A. Maiti, G.E. Overturf, and L.E. Fried, *The Microstructure of TATB-based Explosive Formulations During Temperature Cycling Using Ultra-small Angle X-ray Scattering.* Propellants Explosives Pyrotechnics, 2009. **34**(5): p. 406-414.
2. Kinney, J.H., T.M. Willey, and G.E. Overturf. *On the Nature of Variations in Density and Composition within TATB-based Plastic Bonded Explosives*. in *Proceedings of the 13th International Detonation Symposium.* 2006. Norfolk, VA, USA.
3. Willey, T.M., L. Lauderbach, F. Gagliardi, B. Cunningham, K.T. Lorenz, J.R.I. Lee, T. van Buuren, R. Call, L. Landt, and G.E. Overturf. *Comprehensive Characterization of Voids and Microstructure in TATB-based Explosives from 10 nm to 1 cm: Effects of Temperature Cycling and Compressive Creep*. in *14th International Detonation Symposium*. 2010. Coeur d'Alene, Idaho.
4. http://www.cxro.lbl.gov. Available from: http://www.cxro.lbl.gov.
5. Thompson, D.G., G.W. Brown, J.T. Mang, R. DeLuca, B. Patterson, and S. Hagelberg. *Characterizing the Effects of ratchet Growth on PBX 9502*. in *AIP Conference Proceedings, Shock Compression of Condensed Matter 2009*. 2009. AIP.